Supplementary Material

MoS_2@CoFe-MOF catalysts by one-pot hydrothermal synthesis enhanced electron interaction between MoS_2 nanoflower and bimetallic MOF for efficient oxygen evolution

Jiahui Li, Yufen Wang, Qinyuan Yu, Xuedong Wei*
Key Laboratory of Magnetic Molecules & Magnetic Information Materials Ministry of Education, School of Chemistry & Material Science, Shanxi Normal University, Taiyuan 030031, PR China.

Table of contents

Supplementary Figures

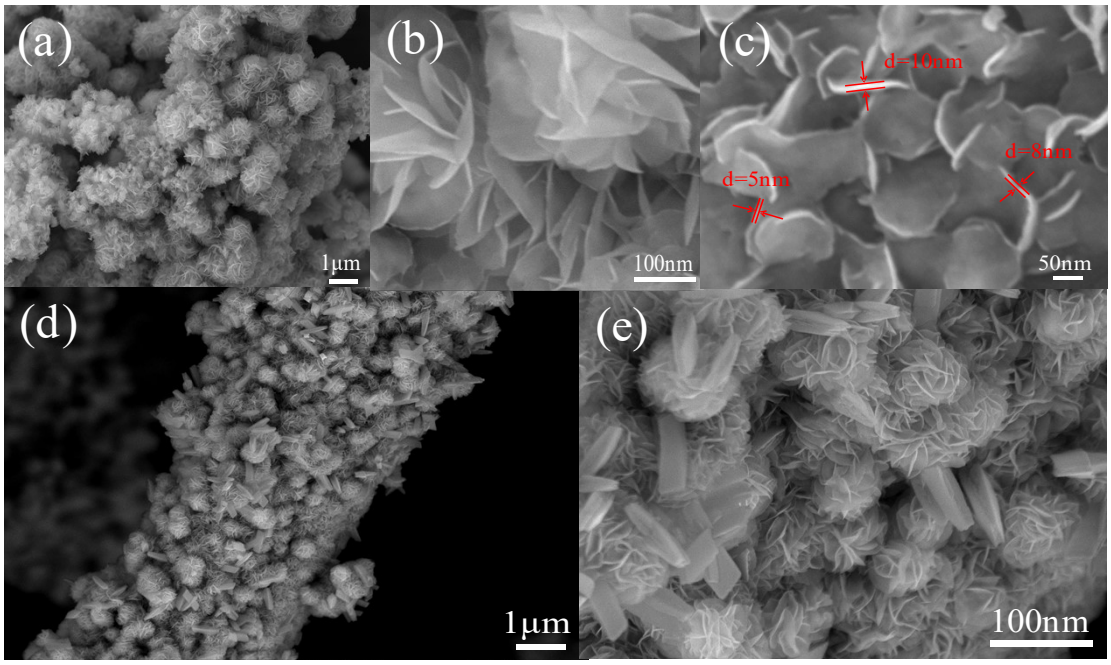

Fig. S1. (a-c) SEM images of the MoS_2, (d-e) SEM images of the MoS_2@Co-MOF(CC).

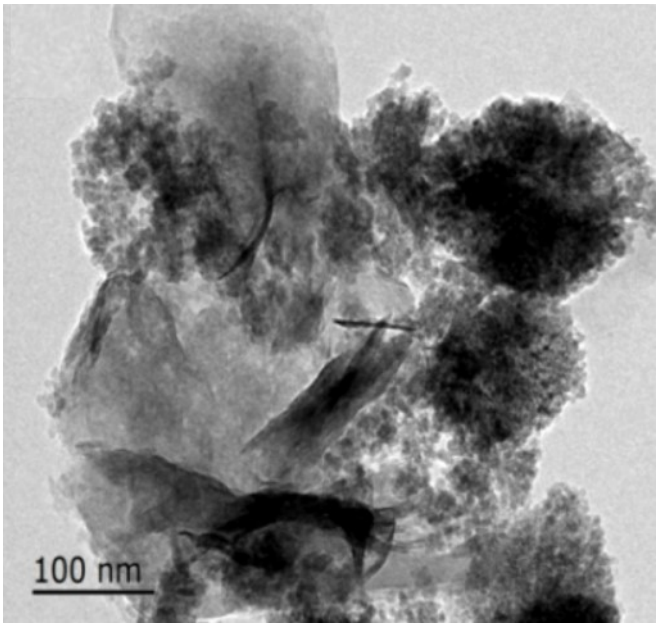

Fig. S2. TEM images of the MoS_2@CoFe-MOF.

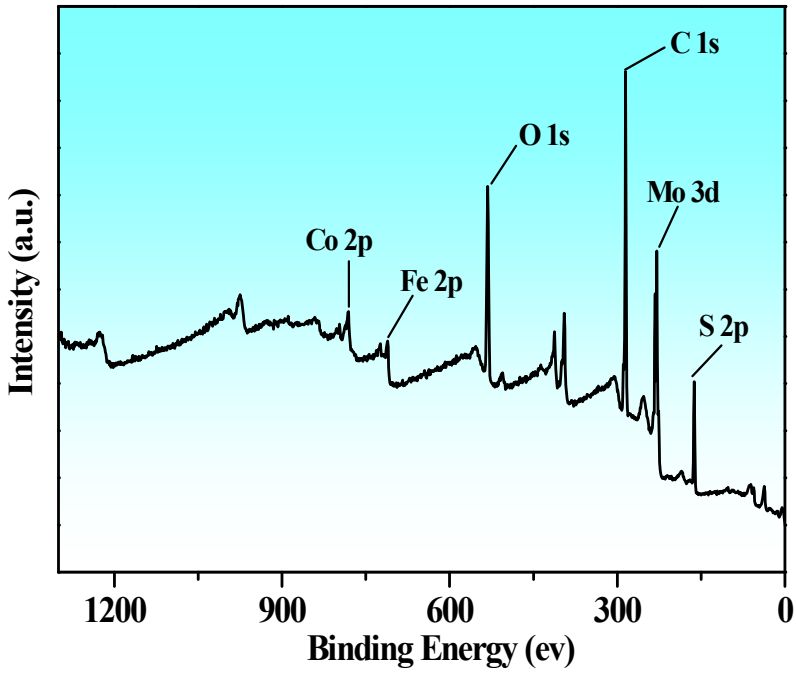

Fig. S3. (a) The XPS survey of the MoS_2@CoFe-MOF(CC).

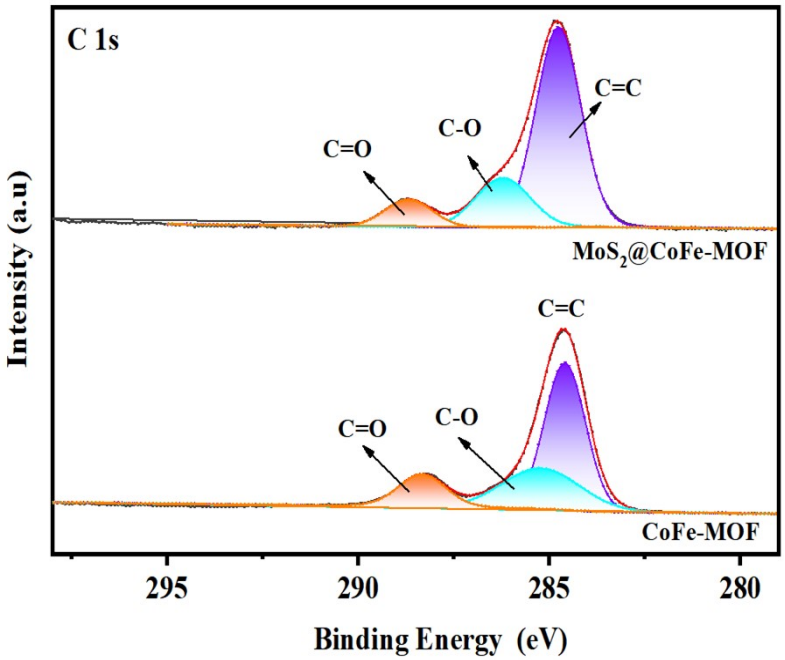

Fig. S4. XPS spectra of C 1s in MoS_2@CoFe-MOF and CoFe-MOF.

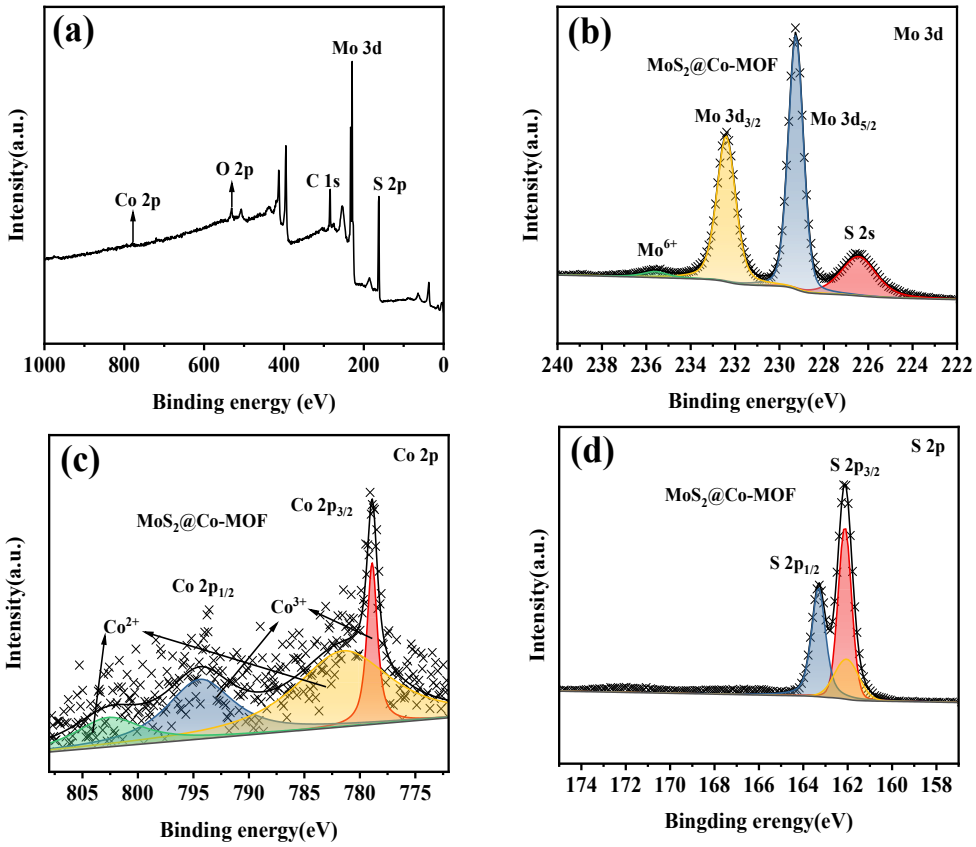

Fig. S5. MoS_2@Co-MOF(CC): (a) XPS full spectra, (b-d) XPS spectra of Mo 3d, Co 2p, S 2p.

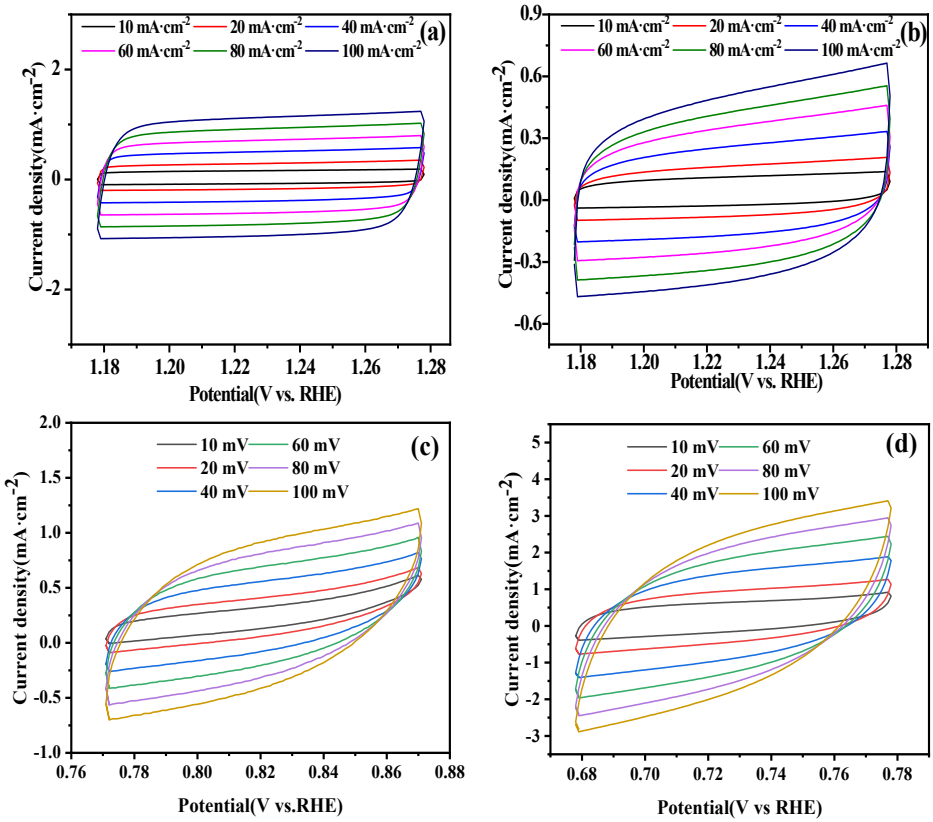

Fig. S6. CV curve of the non-Faraday voltage range (a) CoFe-MOF(CC), (b) MoS_2(CC), (c) MoS_2@Co-MOF(CC), (d) MoS_2@Fe-MOF(CC).

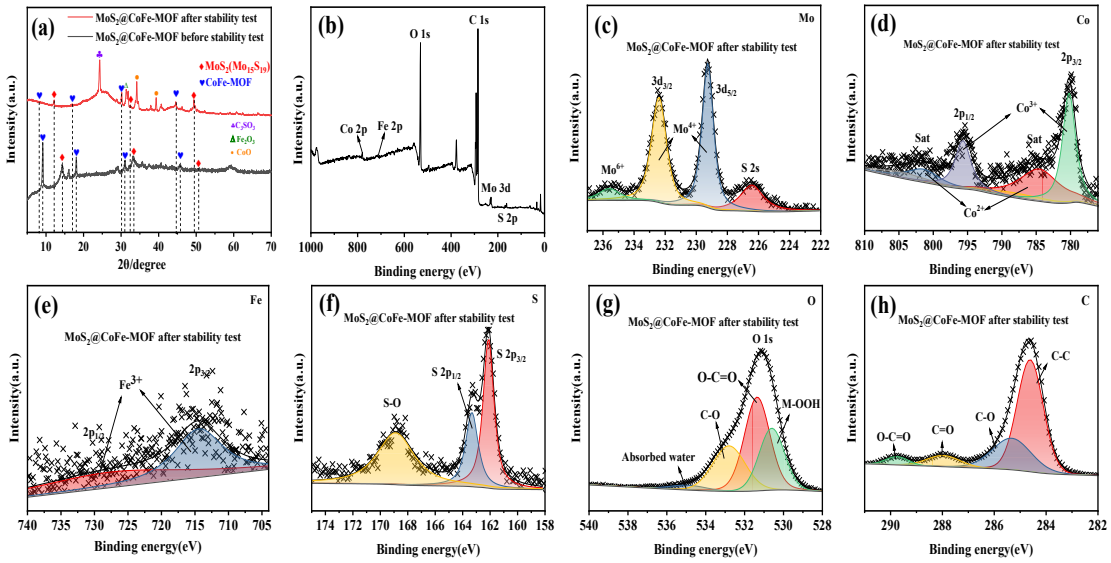
(a)
MoS2@CoFe-MOF after stability test
MoS2@CoFe-MOF before stability test
MoS2(Mo15S19)
CoFe-MOF
C-SO3
Fe2O3
CoO
Intensity(a.u.)
2θ/degree
(b)
O 1s
C 1s
Co 2p
Fe 2p
Mo 3d
S 2p
Intensity(a.u.)
Binding energy (eV)
(c)
Mo
MoS2@CoFe-MOF after stability test
3d3/2
3d5/2
Mo6+
Mo4+
S 2s
Intensity(a.u.)
Binding energy(eV)
(d)
Co
MoS2@CoFe-MOF after stability test
2p3/2
2p1/2
Co3+
Sat
Sat
Co2+
Intensity(a.u.)
Binding energy(eV)
(e)
Fe
MoS2@CoFe-MOF after stability test
Fe3+
2p3/2
2p1/2
Intensity(a.u.)
Binding energy(eV)
(f)
S
MoS2@CoFe-MOF after stability test
S 2p3/2
S 2p1/2
S-O
Intensity(a.u.)
Binding energy(eV)
(g)
O
MoS2@CoFe-MOF after stability test
O 1s
O-C=O
C-O
M-OOH
Absorbed water
Intensity(a.u.)
Binding energy(eV)
(h)
C
MoS2@CoFe-MOF after stability test
C-C
C-O
C=O
O-C=O
Intensity(a.u.)
Binding energy(eV)

Fig. S7. MoS_2@CoFe-MOF(CC) after the stability test: (a) XRD patterns, (b) XPS spectra, (c-h) XPS spectra of Mo 3d, Co 2p, Fe 2p, S 2p, O 1s and C1s.

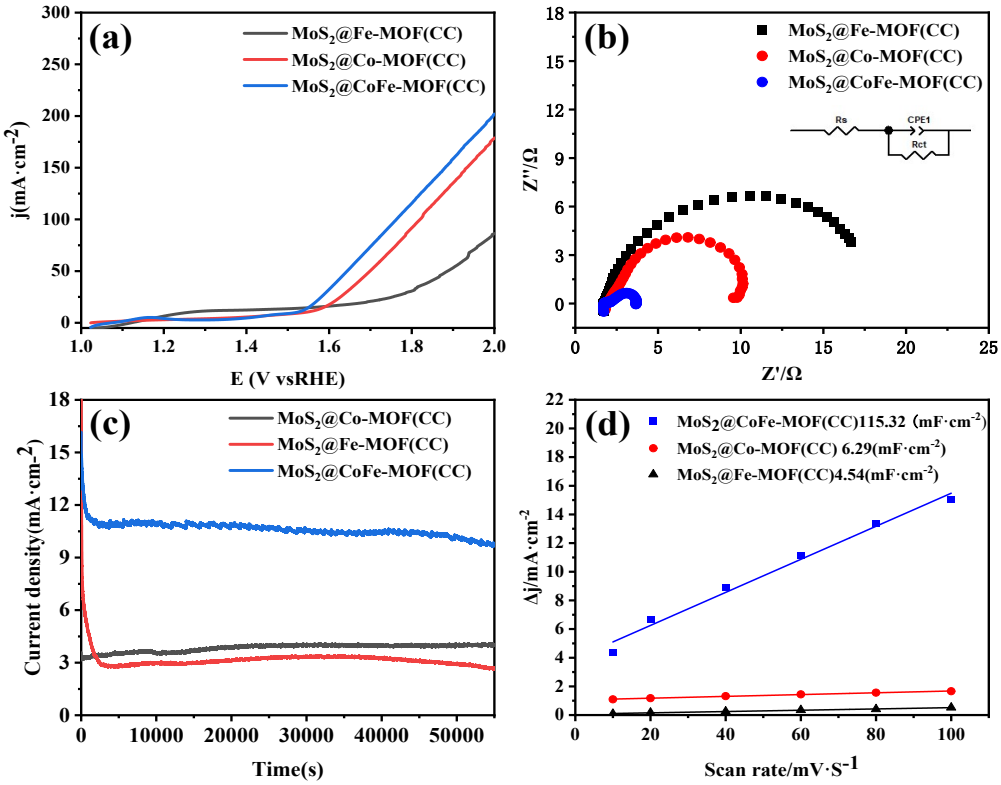

Fig. S8. MoS_2@Fe-MOF(CC), MoS_2@Co-MOF(CC), MoS_2@CoFe-MOF(CC): (a) LSV curves, (b)Electrochemical impedance diagram, (c)Stability test curves, (d)Plots of the current density difference (Δj = ja-jc) at the central potential of the potential window (vs. RHE) against the scan rate.

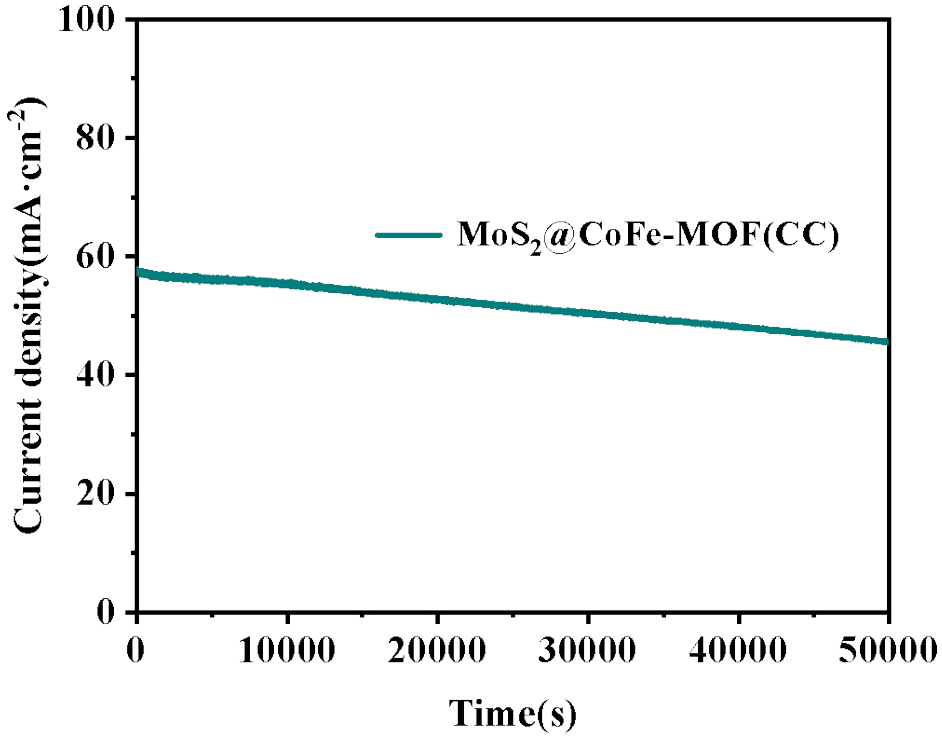

Fig. S9. Stability test curves of MoS_2@CoFe-MOF(CC) at 50 mA·cm^{-2}.

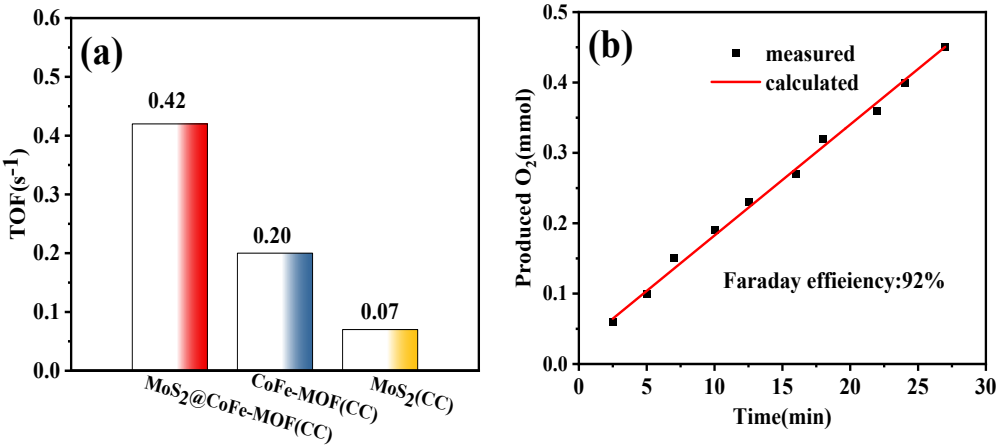

Figure S10. (a) The TOFs of different catalysts at the overpotentials of 220 mV, (b) Gas production measured by drainage.

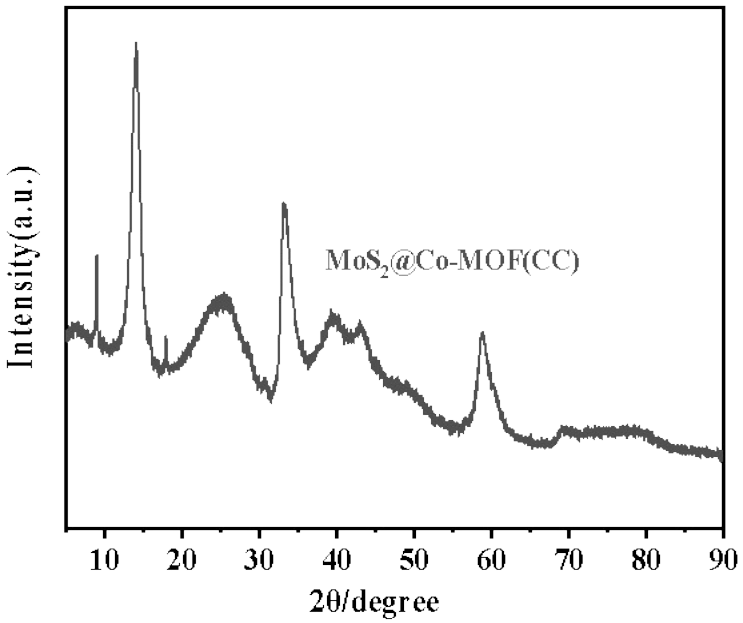

Figure S11. (a) XRD patterns of MoS2@Co-MOF.

Table S1 Comparison of alkaline OER performance with other previously reported transition metal-based electrocatalysts.

Electrocatalysts	Electrolyte	Substrate	Overpotential (10 mA· cm^{-2})	Tafel slope [mV·dec^{-1}]	Ref
MoS_2@CoFe-MOF	1 M KOH	CC	220mV	18.04	This work
$(Ni_2Co_1)_{0.925}Fe_{0.075}$-MOF	1 M KOH	GCE	257mV	41.3	1
FeCo-MNS-1.0	0.1 M KOH	Pt-foil	298mV	21.6	2
CoMoSeS	1 M KOH	CC	375mV	60	3
MoS_2 Nano Islands	1 M KOH	GCE	300mV	45	4
CoFe-MOF	1 M KOH	GCE	265mV	44	5
CoFe/C-650	1 M KOH	GCE	246mV	45.27	6
MoS_2	1 M KOH	NF	320mV	44	7
Co, Nb-MoS_2/TiO_2	1 M KOH	NF	260mV	81.2	8
$CoFeO_x(OH)_y$/MoS_2/CP (CFOMS/CP)	1 M KOH	CC	242mV	37.9	9
CoMoS	1 M KOH	CC	370mV	45	10

Table S2 Elements content comparison from XPS and EDS methods of MoS_2@CoFe-MOF sample.

Test Method	XPS	EDS
Spectrum	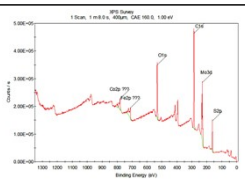	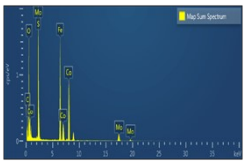
Element	at%	at%
C	52.53	16.01
O	19.43	41.50
Fe	1.85	4.27
Co	8.57	17.02
S	12.36	12.68
Mo	5.26	8.52
Total:	100.00	100.00

References

[1] Q. Qian, Y. Li, Y. Liu, L. Yu and G. Zhang, Ambient fast synthesis and active sites deciphering of hierarchical foam-like trimetal–organic framework nanostructures as a platform for highly efficient oxygen evolution electrocatalysis, Adv. mater., 2019, 31, 1901139.

[2] L. Zhuang, L. Ge, H. Liu, Z. Jiang, Y. Jia, Z. Li, D. Yang, R. K. Hocking, M. Li, L. Zhang and X. Wang, A surfactant-free and scalable general strategy for synthesizing ultrathin two-dimensional metal–organic framework nanosheets for the oxygen evolution reaction, Angew. Chem., 2019, 131, 13699-13706.

[3] B. K. Martini, L. S. Bezerra, S. Artemkina, V. Fedorov, P. K. Boruah, M. R. Das and G. Maia, Efficient OER nanocomposite electrocatalysts based on Ni and/or Co supported on $MoSe_2$ nanoribbons and MoS_2 nanosheets, Chem. Eng. J. Adv., 2022, 9, 100206.

[4] B. Chen, P. Hu, F. Yang, X. Hua, F.-F. Yang, F. Zhu, R. Sun, K. Hao, K. Wang and Z. Yin, In situ porousized MoS2 nano islands enhance HER/OER bifunctional electrocatalysis, Small, 2023, 19, 2207177.

[5] Z. Zou, T. Wang, X. Zhao, W.-J. Jiang, H. Pan, D. Gao and C. Xu, Expediting in-situ electrochemical activation of two-dimensional metal–organic frameworks for enhanced OER intrinsic activity by iron incorporation, ACS Catal., 2019, 9, 7356-7364.

[6] K. Srinivas, Y. Chen, Z. Su, B. Yu, M. Karpuraranjith, F. Ma, X. Wang, W. Zhang and D. Yang, Heterostructural $CoFe_2O_4$/CoO nanoparticles-embedded carbon nanotubes network for boosted overall water-splitting performanc, Electrochim. Acta, 2022, 404, 139745.

[7] B. J. Rani, S. S. Pradeepa, Z. M. Hasan, G. Ravi, R. Yuvakkumar and S. I. Hong, Supercapacitor and OER activity of transition metal (Mo, Co, Cu) sulphides, J. Phys. Chem. Solids, 2020, 138, 109240.

[8] D. C. Nguyen, T. L. L. Doan, S. Prabhakaran, D. T. Tran, D. H. Kim, J. H. Lee and N. H. Kim, Hierarchical Co and Nb dual-doped MoS_2 nanosheets shelled micro-TiO_2 hollow spheres as effective multifunctional electrocatalysts for HER, OER, and ORR, Nano Energy, 2021, 82, 105750.

[9] C. Zhao, X. Zhang, S. Xu, G. Yang, J. Fan, J. Guo, W. Cai and C. Zhao, Construction of amorphous $CoFeO_x(OH)_y/MoS_2$/CP electrode for superior OER performance, Int. J. Hydrogen Energy, 2022, 47, 28859-28868.

[10] J. Hou, B. Zhang, Z. Li, S. Cao, Y. Sun, Y. Wu, Z. Gao and L. Sun, Vertically aligned oxygenated-CoS_2–MoS_2 heteronanosheet architecture from polyoxometalate for efficient and stable overall water splitting, ACS Catal., 2018, 8, 4612-4621.